

Sedimentation and precipitation of nanoparticles in power-law fluids

Liancun Zheng · Botong Li · Ping Lin ·
Xinxin Zhang · Chaoli Zhang · Bin Zhao ·
Tongtong Wang

Received: 19 September 2012 / Accepted: 21 November 2012 / Published online: 15 December 2012
© Springer-Verlag Berlin Heidelberg 2012

Abstract Our experiment reported here adopts water, alcohol (100 %), carboxymethyl cellulose (CMC) aqueous solution with different concentrations as the base-fluid of nano-fluids. We show diffusion, aggregation and precipitation of nano-size particles in the optical quartz glass Petri dishes filled with nano-fluids flat with the help of a rotating cone. The experimental results illustrate that nanoparticles are preferably suspended in CMC aqueous solution than in water or alcohol, which means the effective Hamaker constant of water- or alcohol-particle suspensions is bigger than that of CMC-particle suspension. In the experiment with CMC as the base solution, increasing the viscosity of the solution can alleviate the settling velocity of particles and make the suspension better. The experiment also discovers that in static condition, the mutual attractive force between nanoparticles plays an important role in the suspension; however, if external forces, which are higher than the attraction, exist, they are decisive parts. In addition, Al_2O_3 solution is much more sensitive than the Cu solution with the varying concentration and status in the experiment because the density of Al_2O_3 particles is smaller than that of Cu-nanoparticles.

Keywords Nanofluids · Power-law fluids · Sedimentation · Precipitation · Diffusion

1 Introduction

A wide variety of industries and scientific research depend on the understanding of diffusion–reunion–precipitation of nano size particles to monitor and control product manufacturing processes and their quality, as in fields of metallic powders, pharmaceuticals (Mahmoudi et al. 2011), foods, cosmetics, pollution control (Rissler et al. 2012), ceramics and other materials (Calvin 1993; Goyon et al. 2008; Mattsson et al. 2009). The release of medicine in the body can be regarded as a function of distribution and sedimentation of pharmaceuticals (Jaganathan et al. to be published). Taste and texture of many foods and drinks (Naithier-Dufour et al. 1993), which can be seen as nano-fluids, are primitively related to the diffusion–reunion of the particles they consist of. Since behaviours of particles are critical in two-phase combustion, knowledge of the particle distribution is a key parameter in fossil fuel (Holve et al. 1981; Bonin and Queiroz 1996) systems of aviation. Measurements of nano-size particles distributions in clouds are draw much attention of meteorologists (Shantz et al. 2012). Particle migration is shown to be an important mechanism in either enhancement or deterioration in the forced convective heat transfer of nanofluids. Enhancement of the boiling heat transfer is also observed sensitive to the concentration change of nanofluids (Ding et al. 2007a, b). In this article, we choose laser-based speckle technique (Barth 1984; Black et al. 1996; Mojarad and Krishnan 2012) for studying of diffusion, aggregation and precipitation of nano-particles in optical quartz glass Petri dishes with the help of rotating cone (Ming et al. 2011). Inspired by some

L. Zheng (✉) · B. Li · B. Zhao · T. Wang
School of Mathematics and Physics, University of Science and Technology Beijing, Beijing 100083, China
e-mail: liancunzheng@ustb.edu.cn

B. Li · X. Zhang · C. Zhang
School of Mechanical Engineering, University of Science and Technology Beijing, Beijing 100083, China

P. Lin
Department of Mathematics, University of Dundee,
Dundee DD1 4HN, UK

recent attempts involving non-Newtonian nano-fluids (Niu et al. 2012), we choose both Newtonian fluids and power-law fluids to be the base-fluids of nano-particles.

2 Experimental device and design

This innovative self-design experiment consists of: a laser light source, a group of beam expanding lens, optical quartz glass Petri dishes, CCD fast imaging system and a rotating platform. Laser and the lens are fixed by a customized mechanical optical frame on a shock-proof bed. Rotating platform system is composed by a ZK100 single-axis motion controller and a rotating circular platform, on which the Petri dish is placed (see Fig. 1a).

The nanoparticles were Cu of 100 nm diameter and Al_2O_3 of 20 nm diameter. Figure 1b shows agglomeration of nanoparticles under microscope; while Fig. 1c demonstrates how to measure the size of nanoparticles using a microsurgery ruler. In the case of Cu, the agglomerations of nano-powder are 3–9 mm in diameter. The green laser emitted by LED semiconductor laser is transformed into planar light after going through the lens group. It casts into the Petri dish vertically, beneath which the high-speed image recording system records the speckled pictures. Rayleigh (Yang et al. 2009) scattering is observed. The intensity is inversely proportional to λ^4 in Rayleigh scattering: $I(\lambda)_{\text{scattering}} \propto \frac{I(\lambda)_{\text{incident}}}{\lambda^4}$. λ is the incident light wavelength while $I(\lambda)_{\text{incident}}$ is the incident light intensity distribution function. The light with a short wavelength scatters easily. We chose green laser in this experiment since the wavelength of green light is shorter than that of red light.

According to the classic Rayleigh scattering model, nanoparticles are closely related to the speckles. The distribution and motion of nanoparticles can be deduced by

the corresponding speckles in different moments. When the volume percentage of nanoparticles in fluids is appropriate and suspended with proper mutually distance, the requirements of spatial coherence are satisfied. Through the complex amplitude superposition, the light intensity is re-distributed when the scattering light of particles is interfered. At the same time, high-speed image recording system records clear speckle images with dark and small bright spots. Due to the small height of Petri dish and nano-fluids, the solution can be approximated as a sheet of laminar flow. This sheet, which can be viewed as a diffraction screen consisting of a base-fluid and nanoparticles, is irradiated by the laser beam. Speckle images are observed by the high-speed image recording system below.

The base-fluid of nano-fluids adopted in this experiment was power-law fluids (i.e. carboxymethyl cellulose aqueous solution), as well as Newton fluids (water and alcohol). This experiment first investigates systematically on the motion–diffusion–precipitation characteristics of nano-fluids based on power-law fluid.

3 Experimental results and discussion

Figure 2 shows the laser speckle images of nanoparticles in different solutions. In these three images, Fig. 2c owns the brightest and shapely speckles; Fig. 2a ranks the second; Fig. 2b presents the darkest speckles. Since the brightness of speckles is directly proportional to the number of nanoparticles in suspension, the Cu-nanoparticles with 0.0002 % volume fraction are preferably suspended in CMC aqueous solution than in alcohol. It means that CMC aqueous solution is capable of carrying more Cu-nanoparticles, but in alcohol, the majority of nanoparticles are precipitated down.

The Hamaker constant A is an important material parameter measuring the free energy on particle surface. The effective Hamaker constant of suspension $A_{\text{eff}} = (A_{\text{particle}}^{1/2} - A_{\text{fluid}}^{1/2})^2$ expresses Van Der Waals gravity between particles. A_{particle} is the Hamaker constant of particles, while A_{fluid} is the Hamaker constant of water. When the same particles are suspended in water or alcohol, the effective Hamaker constant of water-particle suspension is smaller than that of alcohol-particle suspensions. The trend of agglomeration in water is relatively weak. It explains why the water-particle suspension is more stable than the alcohol-particle suspensions. Since the water-particle suspension is less stable than CMC-particle suspension, the effective Hamaker constant of water-particle suspensions is bigger than that of CMC-particle suspension. Thereby, we can get $A_{\text{water}} < A_{\text{CMC}}$. A preliminary understanding of the Hamaker constant of CMC aqueous solution is acquired through this experiment.

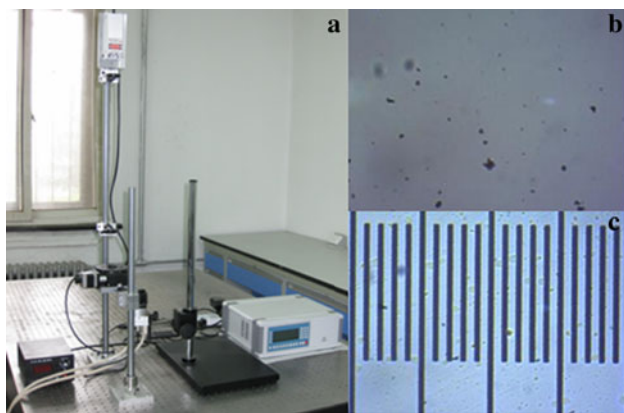


Fig. 1 Experimental device and nano-solutions. **a** Device to detect speckles formed by laser irradiation into nano-fluids; **b**, **c**, Copper powder agglomerate of 3–9 mm diameter in water

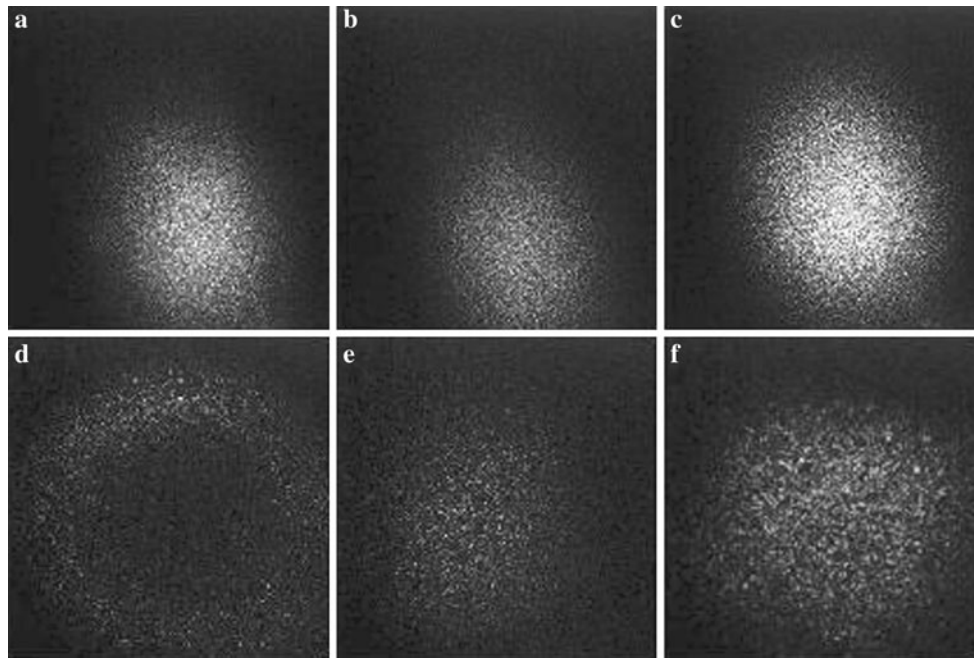


Fig. 2 Laser speckle images of nano-fluids with different based liquid in Petri dish and on glass. The diameter of Cu-nanoparticles is 100 nm. The laser speckle images of nanoparticles in different solutions. **a** Image of suspended in the water; **b** In pure alcohol; **c** In CMC aqueous solution, where the volume fraction of Cu-particles is

0.0002 %; the mass fraction of CMC is 0.01 %; Laser speckle images of nano-fluids with different based liquid on glass. **d** Picture of Cu-nanoparticles suspended in the water; **e** In a pure alcohol; **f** In CMC aqueous solution. The concentration of Cu-nanoparticles is 0.15 M, while the mass fraction of CMC is 1.5 %

As a result of the small height, the nanometre solution in Petri dish can be regarded as a thin layer, wherein the gravity and buoyancy plays a role on suspension of nanoparticles. To eliminate the influence of buoyancy and gravity, the authors spread different nano-solution on a glass slide to repeat the experiment stated above. The influencing factor on the suspension is the viscosity of the base liquid. Three images of Fig. 2d–f share the same phenomena with Fig. 2a–c to demonstrate the conclusion once more: CMC aqueous solution is capable of carrying more Cu-nanoparticles when the concentration of Cu nanoparticles is 0.15 M.

In order to ensure the reliability of experiments, the ultrasonic dispersion method is used in preparation process to disperse nanoparticles, i.e. we put the nano-fluid on the ultrasonic field to remove the mutual attraction between nanoparticles and interactions between particles and molecular of the base liquid. The stability and quantity of suspended nanoparticles are determined by the comprehensive effects of interaction forces between nanoparticles, nanoparticles and the base liquid.

Figure 3 displays speckle images of aqueous solution with different mass fraction CMC mixed with Al_2O_3 of 0.1 % mass fraction. We present a comparison of speckle images under three conditions. Among them, Fig. 3b, e show that after 20 min kept still, these speckles darken because part of particles sink due to the quality, and the

number of particles suspended in the fluids is reducing; Fig. 3c, f demonstrate speckles become brighter and better-proportioned after fluid being rotated for 20 min at 2/35 rad/s.

It is well-known that the laser transmittance (which also can be seen as the speckle image quality) is influenced by the distribution of suspended particles, in addition to the volume percentage of nanoparticles in the fluids. Rayleigh scattering, which is scattering of light caused by particles much smaller than the wavelength of the light, is the reason to generate speckle images. With more and more serious reunion of nanoparticles, the scattering gets worse. Some researchers (Ding et al. 2006, 2007a, b; Lu et al. 2008) have pointed out that one of the important reasons for the inhomogeneity of nanofluids is the presence of agglomerates due to the attraction between nanoparticles, e.g. Van der Waals attractive force. Mass force (such as gravity) on the assembled particle cluster will be of great influence on their suspension. In static condition, the mutual attractive force between nanoparticles plays an important role in the suspension; however, if external forces, which are higher than the attraction, exist, they are decisive parts. Therefore, in the influence of outside forces, nanoparticles orbit along a certain circular to produce a weakened agglomeration. Even brighter speckle images are obtained afterwards.

Figure 4 shows the speckle images of aqueous solution with 0.01 % mass fractions of CMC and different volume

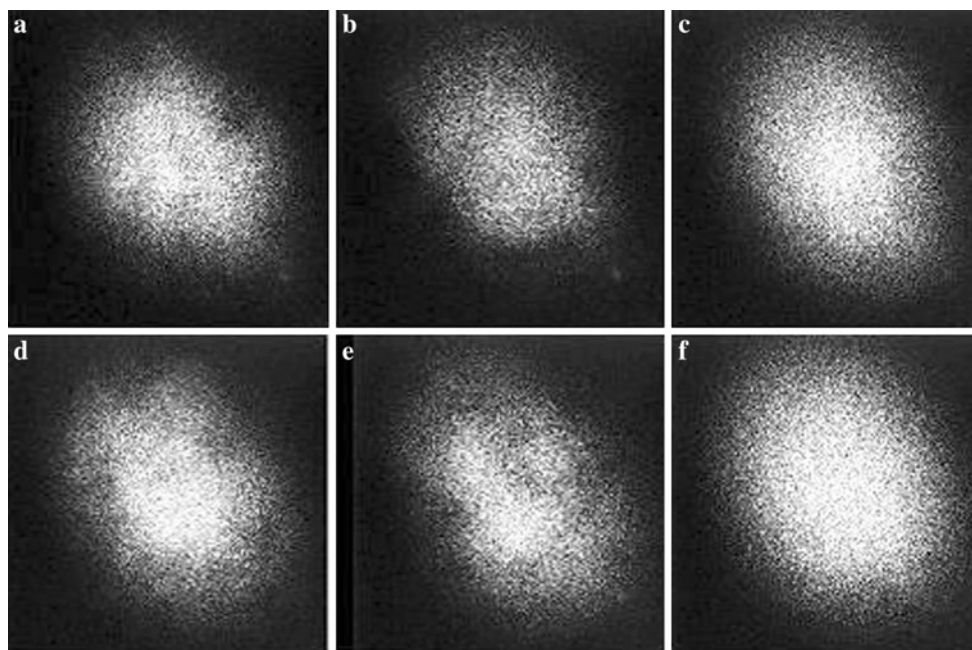


Fig. 3 Speckle images of aqueous solution with different mass fractions of CMC and 0.1 % mass fraction of Al_2O_3 . **a, d**, The solution just removed from the ultrasonic field; **b, e**, Solution placed

in a state of rest for 20 min; **c, f**, Rotated in a particular angular velocity for 20 min. **a–c** Mass fraction of CMC is 0.01 %; **d–f** Mass fraction of CMC is 0.04 %

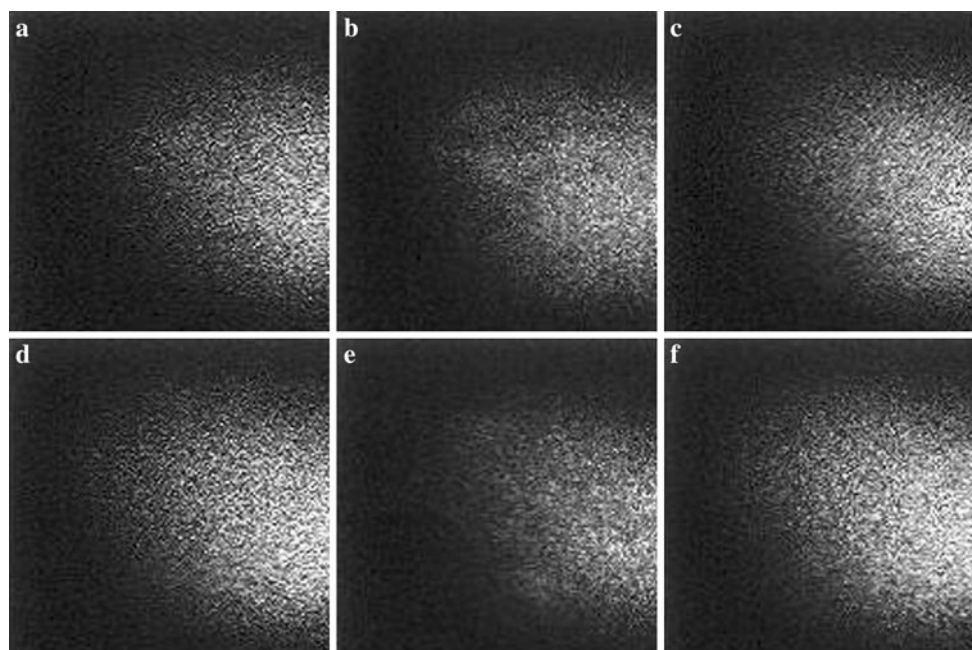


Fig. 4 Speckle images of aqueous solution with 0.01 % mass fractions of CMC and different volume fraction of Cu. Concentration of Cu in **a–c** is 0.03 M, while in **d–f** is 0.04 M. **a, d** Speckle patterns

when nanoparticles have just been removed from the ultrasonic field; **b, e** Particles suspended in the fluids after 20 min; **c, f** Speckle images of nano-solution after being rotated for 20 min at 1/35 rad/s

fraction of Cu. The motion conditions in Fig. 4 are similar to Fig. 3. From Fig. 4, it can be seen that speckle images with a high concentration nano-solution are brighter and more symmetrical than ones with a lower concentration

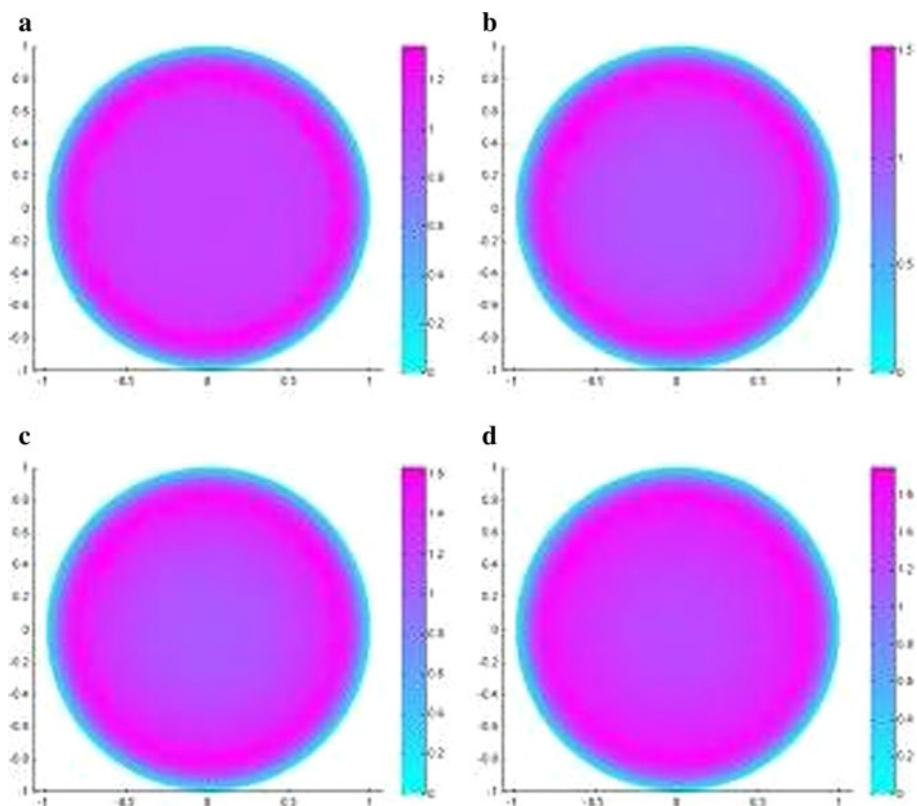
nano-solution. A more interesting phenomenon is, when comparing Figs. 3 and 4, we will find Al_2O_3 solution is much more sensitive than the Cu solution with the varying concentration and status, that is, differences are obvious

between images. This is because the density of Al_2O_3 particles is smaller than that of Cu-nanoparticles. As we all know, the quality force (i.e. gravity, buoyancy) of nanoparticles/particle clusters hold sway over the suspension, and the quality force is significantly influenced by the density of particles. The smaller the density and the sedimentation force are, the higher the suspension stability is.

4 Modelling and numerical analysis

In this section, the author will model for the volume fraction of nanoparticles. We will verify the experimental conclusion through the numerical simulation of particle distribution in nanofluid in a Petri dish under the influence of movement. Pascal (1996) proposed a one-dimensional convection–diffusion model with nonlinear molecular diffusion for mass transfer in a two-phase system. Niu et al. (2012) also adopted the power-law rheology to describe the characteristics of a non-Newtonian nanofluid flow in a microtube theoretically. These pioneering works inspired us. In our article, the model of φ is $\varphi_t + u \cdot \nabla \varphi = \text{div}(D_B \nabla C(x, y))$, where $C(x, y) = (\varphi_x^2 + \varphi_y^2)^{\frac{n-1}{2}}$; D_B is the Brownian diffusion coefficient, and n is the power-law index. The volume fraction distribution will be obtained, which will be compared with the experimental images to prove the correctness of the model.

Fig. 6 Images of concentration at different time when $n = 0.85$, $Le = 1.0$, $\omega = \pi/35$. **a**, 100 dt; **b**, 400 dt; **c**, 800 dt; **d**, 1,600 dt



We adopted the continuous finite element method to solve the model using the Freefem++ software. u, v, φ are handled with piecewise P_2 continuous finite element while the pressure p with piecewise linear element (Lin and Liu 2006). The Petri dish with radius of 1 is filled with nanofluid (the base-fluid is a power-law fluid with the

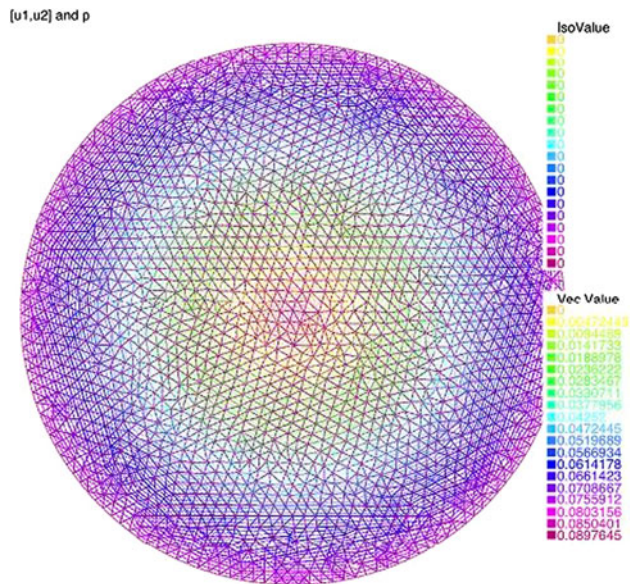


Fig. 5 Calculated grids when $\omega = \pi/35$ rad/s, $n = 0.85$ in the rotating disc with the radius of 1

power-law exponent $n = 0.85$). Figure 5 is drawn with the angular speed $\pi/35$ rad/s. From the graph, it can be seen that the grids are fine enough.

Figure 6 displays images of different times when $n = 0.85$, $\mu_f = 0.01754$, $Le = 1.0$, $\omega = \pi/35$. Figure 6a–d are images with time step size of 100, 400, 800 and 1,600, respectively. Assume that the dish is uniformly filled with nanofluid (base-fluid is power-law fluid with dimensionless concentration $\varphi = 1.0$) at the initial moment, we can find that as time passes, the concentration of solution decreases gradually around the center of the Petri dish, while the suspended nanoparticles by degrees gathered near the circumferential portion of the dish. Concentration of solution progressively becomes larger especially around the region of a radius of 0.8, which is in good agreement with the experimental results. The rotating centrifugal force, which is far greater than the forces between nanoparticles, drives the nanoparticles away from the circle center of the Petri dish, which also can be seen from the changes of concentration.

Figure 7 exhibits speckle images of nanofluid with different power-law base-fluids rotated after 200 dt. In Fig. 7a, the power-law index of base-fluid (water) is $n = 1.0$. From Fig. 7, it can be seen that with the power-law index of base-fluid is lower, the concentration distribution of nanoparticles is more uniform in the speckle images and the high level concentration area by the edge of the disc stretches. The data

of power-law index of base-fluids and consistency coefficient are from (Elyad 2008; Zhang 2008). The carboxymethyl cellulose (CMC) water solution with concentration 0.0–0.4 % can be approximated as the power-law fluids when the power-law index $0 < n < 1$ and the heat capacity, density and thermal conductivity are almost as same as the water. The viscosity of base-fluid plays an important role in the suspension of nanoparticles. As the viscosity is getting bigger, nanoparticles are less likely to accumulate, and their settlings blunts. According to Stoke's law, settling velocity of particles is $v = \frac{2}{9} \cdot \frac{r^2(\rho_1 - \rho_2)g}{\eta}$ (Lamb 1994), where r is the particle radius, ρ_1 and ρ_2 are density of particles and solution, respectively, and η is the viscosity of solution. From this formula, it can be deduced that, with a bigger viscosity of base-fluid, the deposition rate of nanoparticles is slower, while the suspension of nanoparticles is getting better, and the concentration distribution in the container is more uniform. Comparing with a base liquid owning a smaller viscosity, the concentration of nanoparticles in solution is higher. The experiment is carried out to verify this phenomenon (ref. to Fig. 2).

Images of concentrations in nanofluids with different Le number when $n = 0.85$, $\omega = \pi/35$, 400 dt are drawn in Fig. 8. The Lewis number $Le = \frac{\mu}{\rho_f D_B}$ is a dimensionless number, defined as the ratio of thermal diffusion and mass

Fig. 7 Images of nanofluids with different power-law base liquid when $Le = 1.0$, $\omega = \pi/35$, 200 dt. **a**, $n = 1.0$; **b**, $n = 0.91$; **c**, $n = 0.81$; **d**, $n = 0.76$

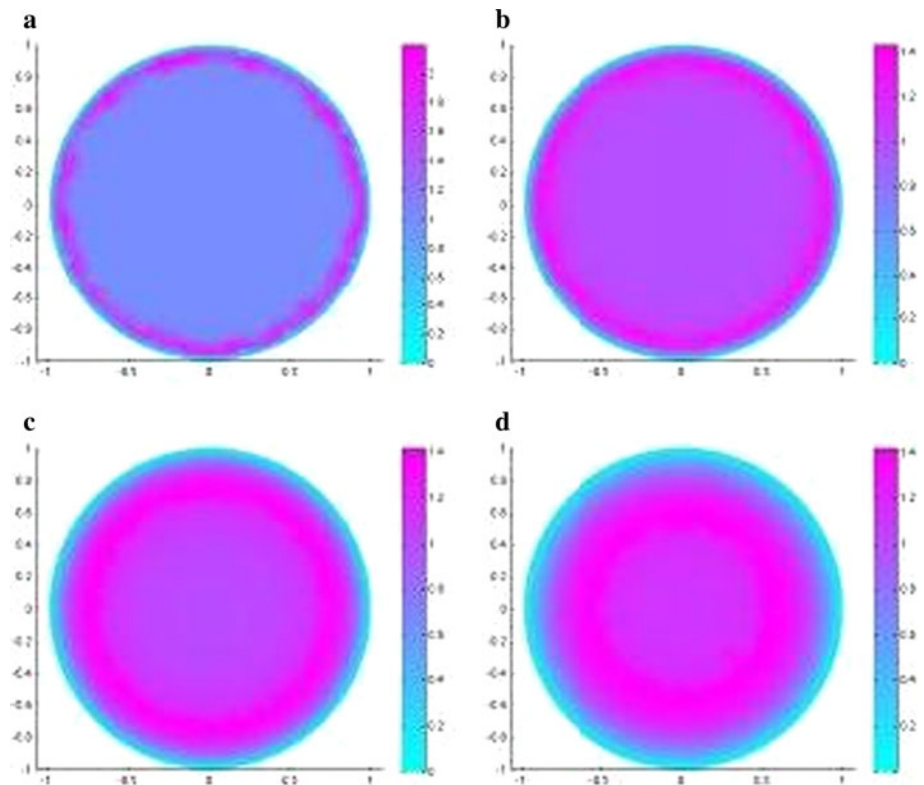
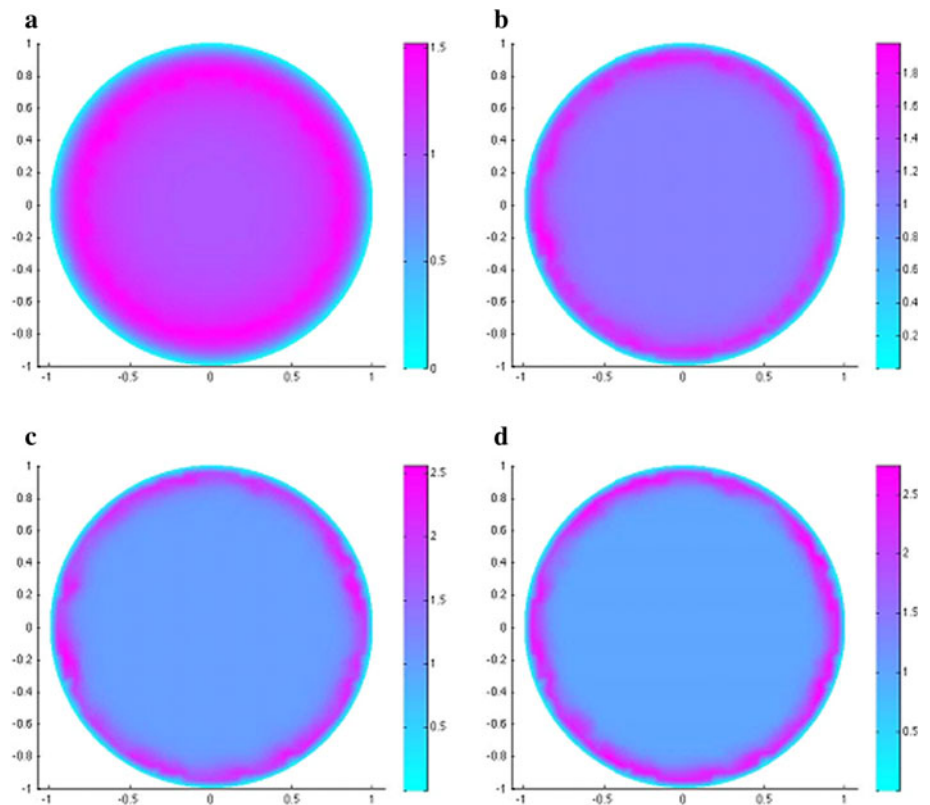


Fig. 8 Images of concentrations in nanofluids with different Le number when $n = 0.85$, $\omega = \pi/35$, 400 dt. **a**, $Le = 1.0$; **b**, $Le = 5.0$; **c**, $Le = 9.0$; **d**, $Le = 13.0$



diffusion coefficient, which characterizes the heat and mass transfer in convective fluid flow (in this article $1 < Le < 25$) (Noghrehabadi et al. 2012). The larger the Le number is, the more strongly the effect of mass transfer is. Figure 8 reveals that, with a larger Le number, the concentration of nanoparticles by the edge of disc is greater, and nanoparticles cluster fast with the rotation of the disc. It might be concluded that the Le number characterizes the speed of nanoparticles aggregation as well.

Acknowledgments The study is supported by the National Natural Science Foundations of China (No. 51076012, 51276014).

References

- Barth HG (1984) Modern methods of particle size analysis. Wiley, New York
- Black DL, McQuay MQ, Bonin MP (1996) Laser-based techniques for particle-size measurement: a review of sizing methods and their industrial applications. *Prog Energy Combust Sci* 22: 267–306
- Bonin MP, Queiroz M (1996) A parametric evaluation of particle-phase dynamics in an industrial pulverised. *Fuel* 75:195–206
- Calvin GJ (1993) Field-flow fractionation-analysis of macromolecular, colloidal and particulate materials. *Science* 260:1456–1465
- Ding YL, Alias H, Wen DS, Williams RA (2006) Heat transfer of aqueous suspensions of carbon nanotubes (CNT nanofluids). *Int J Heat Mass Transf* 49:240–250
- Ding YL, Chen HS, He YR, Lapkin A, Butenko Y (2007a) Forced convective heat transfer of nanofluids. *Adv Powder Technol* 18(6):813–824
- Ding YL, Chen HS, Wang L, Yang CY, He YR, Yang W, Lee WP, Zhang LL, Hu R (2007b) Heat transfer intensification using nanofluids. *KONA* 25:23–38
- Elyad AN (2008) Application of nanofluids for heat transfer enhancement of separated flows encountered in a backward facing step. *Int J Heat Fluid Flow* 29:242–249
- Goyon J, Colin A, Ovarlez G, Ajdari A, Bocquet L (2008) Spatial cooperativity in soft glassy flows. *Nature* 454:84–87
- Holve DJ, Tichenor D, Wang JCF, Hardesty DR (1981) Design criteria and recent developments of optical single particle counters for fossil fuel systems. *Opt Eng* 20:529–539
- Jaganathan H, Godin B (2012) Biocompatibility assessment of Si-based nano- and micro-particles. *Adv Drug Delivery Rev*. doi: 10.1016/j.addr.2012.05.008
- Lamb H (1994) *Hydrodynamics*. Cambridge University Press, Cambridge
- Lin P, Liu C (2006) Simulations of singularity dynamics in liquid crystal flows: a C^0 finite element approach. *J Comput Phys* 215:348–362
- Lu PJ et al (2008) Gelation of particles with short-range attraction. *Nature* 453:499–504
- Mahmoudi M, Sant S, Wang B, Laurent S, Sen T (2011) Superparamagnetic iron oxide nanoparticles (SPIONs): development, surface modification and applications in chemotherapy. *Adv Drug Delivery Rev* 63:24–46
- Mattsson J, Wyss HM, Fernandez-Nieves A, Miyazaki K, Hu Z (2009) Soft colloids make strong glasses. *Nature* 462:83–86
- Ming CY, Zheng LC, Zhang XX (2011) Steady flow and heat transfer of the power-law fluid over a rotating disk. *Int Commun Heat Mass Transf* 38:280–284

- Mojarad N, Krishnan M (2012) Measuring the size and charge of single nanoscale objects in solution using an electrostatic fluidic trap. *Nature* 7:448–452
- Naithier-Dufour N, Bougeard L, Devaux M, Bertrand DL, Deschault F (1993) Comparison of sieving and laser diffraction for the particle size measurements of raw materials used in foodstuff. *Powder Technol* 76:191–200
- Niu J, Fu C, Tan W (2012) Slip-flow and heat transfer of a non-Newtonian nanofluid in a microtube. *PLoS ONE* 7(5):e37274
- Noghrehabadi A, Pourrajab R, Ghalambaz M (2012) Effect of partial slip boundary condition on the flow and heat transfer of nanofluids past stretching sheet prescribed constant wall temperature. *Int J Therm Sci* 54:253–261
- Pascal JP (1996) Effects of nonlinear diffusion in a two-phase system. *Physica A* 223:99–112
- Rissler J et al (2012) Experimental determination of deposition of diesel exhaust particles in the human respiratory tract. *J Aerosol Sci* 48:18–33
- Shantz NC et al (2012) Cloud condensation nuclei droplet growth kinetics of ultrafine particles during anthropogenic nucleation events. *Atmos Environ* 47:389–398
- Yang AHJ et al (2009) Optical manipulation of nanoparticles and biomolecules in sub-wavelength slot waveguides. *Nature* 457:71–75
- Zhang H (2008) A study of the boundary layer on a continuous moving surface in power law fluids. Dissertation, University of Science and Technology Beijing, Beijing, China